Accepted Article

DR. NICHOLAS JONES (Orcid ID : 0000-0003-4846-5117)

Article type : Original Article: Basic and Translational Allergy Immunology

Title: Interleukin-5 drives glycolysis and reactive oxygen species-dependent citric acid cycling by eosinophils

Authors: Nicholas Jones[1], Emma E. Vincent [2,3], Lindsey C. Felix[4], James G. Cronin[1], Louis M. Scott[1], Paul S. Hole[5], Paige Lacy[4] and Catherine A. Thornton[1,*]

Affiliations: [1]Institute of Life Science, Swansea University Medical School, Swansea, SA2 8PP, United Kingdom. [2]MRC Integrative Epidemiology Unit, University of Bristol, Oakfield House, Bristol, BS8 2BN, United Kingdom. [3]Cellular and Molecular Medicine, University of Bristol, Biomedical Sciences Building, Bristol, BS8 1TD, United Kingdom. [4]Alberta Respiratory Centre (ARC), Department of Medicine, University of Alberta, Edmonton, Alberta, T6G 2G3 Canada. [5]Department of Haematology, Division of Cancer and Genetics, School of Medicine, Cardiff University, Cardiff, CF14 4XN, United Kingdom.

[*] Corresponding author: Professor Cathy Thornton
Swansea University Medical School
Singleton Park
Swansea
SA2 8PP
E-mail: c.a.thornton@swansea.ac.uk
Telephone: +44 (0) 1792 602122.

Running title: IL-5 drives the eosinophil metabolic response

Word count: 3211

This article has been accepted for publication and undergone full peer review but has not been through the copyediting, typesetting, pagination and proofreading process, which may lead to differences between this version and the Version of Record. Please cite this article as doi: 10.1111/ALL.14158

This article is protected by copyright. All rights reserved

Accepted Article

Abstract

Introduction: Eosinophils have been long implicated in anti-parasite immunity and allergic diseases and, more recently, in regulating adipose tissue homeostasis. The metabolic processes that govern eosinophils, particularly upon activation, are unknown.

Methods: Peripheral blood eosinophils were isolated for analysis of metabolic processes using extracellular flux analysis and individual metabolites by stable isotope tracer analysis coupled to gas chromatography-mass spectrometry following treatment with IL-3, IL-5 or granulocyte-macrophage colony-stimulating factor (GM-CSF). Eosinophil metabolism was elucidated using pharmacological inhibitors.

Results: Human eosinophils engage a largely glycolytic metabolism but also employ mitochondrial metabolism. Cytokine stimulation generates citric acid cycle (TCA) intermediates from both glucose and glutamine revealing this previously unknown role for mitochondria upon eosinophil activation. We further show that the metabolic program driven by IL-5 is dependent on the STAT5/PI3K/Akt signalling axis and that nicotinamide adenine dinucleotide phosphate oxidase (NOX)-dependent ROS production might be a driver of mitochondrial metabolism upon eosinophil activation.

Conclusion: We demonstrate for the first time that eosinophils are capable of metabolic plasticity, evidenced by increased glucose-derived lactate production upon ROS inhibition. Collectively this study reveals a role for both glycolysis and mitochondrial metabolism in cytokine-stimulated eosinophils. Selective targeting of eosinophil metabolism may be of therapeutic benefit in eosinophil-mediated diseases and regulation of tissue homeostasis.

This article is protected by copyright. All rights reserved

Accepted Article

Keywords: eosinophils, glycolysis, IL-5, metabolism, TCA cycle

This article is protected by copyright. All rights reserved

Accepted Article

Introduction

Human eosinophils reside primarily in haematopoietic and mucosal tissues. Interest in eosinophil activity stems predominantly from their role in anti-parasite immunity and allergic disease[1-5] but there is growing interest in their role in tissue homeostasis, especially adipose tissue[6]. Eosinophil-mediated effector function involves degranulation, the release of antimicrobial cytotoxic molecules, and the respiratory burst[2] yet we know little about the immunometabolic processes that underpin these activities. Activation of other granulocyte populations such as neutrophils and mast cells enhances glycolysis to support biosynthetic intermediate production and rapid ATP generation[7,8]. Eosinophil metabolism is assumed to be largely homologous to that of neutrophils, where, despite the presence of mitochondria, energy production stems primarily from glycolysis[5,9,10].

Non-metabolic roles for mitochondria within eosinophils have been the focus of several investigations. Mitochondrial DNA can be released in a 'catapult-like' fashion from eosinophils and contributes to antibacterial defence, although this remains controversial and has yet to be confirmed[11,12]. Furthermore, the initiation of apoptosis has been reported as an alternative role to respiration for eosinophil mitochondria[10]. As eosinophils produce large amounts of nicotinamide adenine dinucleotide phosphate oxidase (NOX)2-dependent extracellular reactive oxygen species (ROS) upon activation[13-15], it is commonly thought that oxygen consumption by eosinophils supports ROS production rather than oxidative phosphorylation (OXPHOS). Contrary to this, human eosinophils are sensitive to oligomycin (mitochondrial ATP synthase inhibitor), suggesting that in addition to glycolysis, mitochondria can indeed contribute, at least in part, to ATP production[5]. As such, the role of the mitochondria in eosinophils remains unclear and requires investigation.

Glycolysis has been reported to be the main source of ATP in numerous cell types[16-18]. This is especially true for immune cells such as T cells and mast cells, which undergo a glycolytic switch upon activation to support rapid ATP production[19,20]. Little is known about the role of glycolysis in eosinophil-mediated immunity, but glycolysis-derived ATP is essential for the removal of schistosomula by human eosinophils[21] and cytokines such as IL-3, IL-5, granulocyte-macrophage colony-stimulating factor (GM-CSF) and TNFα stimulate glucose uptake in these cells[22]. The anti-apoptotic cytokines IL-3, IL-5, and GM-CSF, produced primarily by T cell subsets, fibroblasts,

This article is protected by copyright. All rights reserved

and epithelial cells, are critical for eosinophil activation and maturation[2]. Differential effects of IL-3, IL-5, and GM-CSF have been identified, with IL-3 generally being a weaker inducer of eosinophil activation than either IL-5 or GM-CSF; IL-3 induces less glucose uptake, superoxide production and eosinophil-derived neurotoxin (EDN) release than IL-5 or GM-CSF[22,23]. However, IL-3 can prolong ribosomal protein S6 signalling compared to IL-5 and GM-CSF, producing augmented levels of semaphorin-7A and heightened protein translation[24]. Despite these differences in responses of eosinophils to IL-3, IL-5, and GM-CSF, the impact of these cytokines on human eosinophil metabolic adaptation that underpins these different functional outcomes has not been studied.

Here, for the first time, we demonstrate that human eosinophils are metabolically plastic cells, up-regulating both glycolytic and TCA cycle intermediates upon activation. We show that IL-3, IL-5 and GM-CSF all increase glycolysis and importantly, that upon activation by these cytokines, eosinophils increase glutaminolysis and subsequent TCA cycling. This is significant as these cells were previously thought to not engage their mitochondria for metabolic purposes. In contrast to earlier studies[10], we report that the IL-5-induced metabolic switch initiates glycolysis and enhances mitochondrial respiration in a mechanism that is dependent on the STAT5/PI3K/Akt axis. Finally, the ability of esoinophils to compensate for inhibition of ROS production and the associated reduced levels of TCA cycle intermediates by increased aerobic glycolysis highlights their metabolic plasticity.

Materials and Methods

This article is protected by copyright. All rights reserved

Accepted Article

Human eosinophil isolation

Human peripheral blood was collected from both male (n = 9) and female donors (n = 25) aged between 18-70 years into heparinised Vacuettes™ (Greiner Bio-one, Frickenhausen, Germany). We recruited both atopic and non-atopic donors with eosinophils comprising between 1-8% of total circulating leukocytes. Specific donor demographics can be found in supplementary table 1. All samples were collected with informed written consent and ethical approval was obtained from Wales Research Ethics Committee 6 (13/WA/0190). Eosinophils were isolated by negative selection using immunomagnetic microbeads (autoMACS; Miltenyi Biotec, Cologne, Germany). Detailed Materials and Methods can be found in the online supplement of this article.

Accepted Article

This article is protected by copyright. All rights reserved

Results

Eosinophils increase glycolysis in response to cytokines

In human eosinophils, IL-3, IL-5, and GM-CSF are the predominant cytokines associated with their activation[25]. Therefore, the effect of IL-3, IL-5 and GM-CSF on eosinophil metabolism was investigated.

First, we investigated the mode of glucose transport in eosinophils. Gene expression levels of the main glucose transporters (*GLUT1-4; SLC2A1-4*) were determined using qPCR. While there was donor variability, *GLUT1 (SLC2A1)* and *GLUT3 (SLC2A3)* were expressed by all donors (Figure 1A). *GLUT4 (SLC2A4)* expression was not detected, and only some donors expressed detectable *GLUT2* (SLC2A2; 3/7) (Figure 1A). Uptake of a fluorescent glucose analogue 2-(*N*-(7-nitrobenz-2-oxa-1,3-diazol-4-yl)amino)-2-deoxyglucose (2-NBDG) did not differ between unstimulated and cytokine-stimulated eosinophils (Figure 1B).

To further investigate the induction of glycolysis upon activation in eosinophils, we performed extracellular flux analysis measuring the extracellular acidification rate (ECAR) upon treatment with IL-3, IL-5, or GM-CSF. Eosinophils were starved of glucose, treated with cytokine followed by the reintroduction of glucose, then addition of the ATP synthase inhibitor oligomycin, with a final addition of 2-deoxy-D-glucose (2-DG) to arrest glycolysis over the timeline shown in Figure 1C. Here we discovered that after a period of glucose starvation, IL-5 or GM-CSF treatment increased ECAR significantly in comparison to either the control or IL-3-treated cells (Figure 1C-D). As there are multiple sources of acidification that may contribute to ECAR in eosinophils[26-28], we performed stable isotope tracer analysis (SITA) to determine the fate of glucose-derived carbon atoms upon eosinophil activation. Eosinophils were activated with IL-3, IL-5 or GM-CSF in the presence of $^{13}C_6$-glucose for 4 h. If eosinophil metabolism is largely homologous to that of neutrophils[29], i.e. glycolytic, then it would be expected that the majority of labelled carbon would be present as the m+3 mass isotopologue of lactate produced from the m+3 mass isotopologue of pyruvate (Figure 1E). These data demonstrate that IL-3, IL-5, or GM-CSF treatment promotes the incorporation of ^{13}C atoms into pyruvate (Figure 1F-G) and lactate (Figure 1H-I). We also observed ^{13}C labelled extracellular lactate within the supernatant (Figure 1J), excess production of lactate upon activation was also confirmed by a standard lactate assay (Figure 1K). Collectively

This article is protected by copyright. All rights reserved

the data demonstrate that eosinophils treated with IL-3, IL-5 or GM-CSF switch to a glycolytic metabolism.

Cytokine-stimulated eosinophils consume oxygen for ROS production

It has been reported that eosinophils do not require their mitochondria for ATP production via OXPHOS[10,30]. However, mitochondria are diverse organelles with multiple metabolic roles. We confirmed the presence of mitochondria using transmission electron microscopy (Figure 2A). Mitochondrial function was assessed by measuring oxygen consumption rate (OCR) in the presence of IL-3, IL-5 or GM-CSF (Figure 2B). Baseline OCR was increased in IL-5 and GM-CSF treated cells post-glucose starvation compared to the control and IL-3-treated cells (Figure 2C). We noted a decrease in OCR upon oligomycin treatment under all conditions, this is indicative of oxygen consumption for ATP generation, which is in agreement with a previous study[5]. Increasing the concentration of IL-3 delivered to the cells caused an increase in both ECAR and OCR (50 and 100 ng/mL; Figure 2D-E) suggestive of a differential kinetic response of eosinophils to IL-3 versus IL-5/GM-CSF.

In our experiments, eosinophils clearly consume oxygen, especially in response to treatment with IL-5 or GM-CSF. However, oxygen consumption can occur independently of OXPHOS for processes such as respiratory burst, involving the generation of ROS and subsequently hydrogen peroxide via NOX enzymes[13,14]. To determine whether any of the cytokine-induced oxygen consumption was due to mitochondrial ROS production, we utilised the mitochondrial superoxide indicator MitoSOX and selected a time point to coincide with the extracellular flux assay (15 minutes). Regardless of the cytokine used for stimulation, mitochondria did not contribute to oxygen consumption via ROS production at the time point measured; rotenone was used as a positive control (Figure 2F-G).

To further investigate increased oxygen consumption upon stimulation we investigated whether IL-3, IL-5 and GM-CSF induce total ROS production. We determined total oxidative stress levels using the fluorescent probe CellROX and flow cytometry, phorbol 12-myristate 13-acetate (PMA) was used as a positive control. All three cytokines induced ROS production in comparison to the CellROX control with GM-CSF being the most potent (Figure 2H-I). Using the inhibitor diphenyleneiodonium (DPI), these responses were shown to be NOX-dependent, although this was

This article is protected by copyright. All rights reserved

only significant for GM-CSF and PMA-induced ROS production. These data raise the question of what happens to OCR when ROS production is inhibited, and we have addressed this in relation to IL-5 later in the manuscript, see Figure 5.

Cytokine-stimulated eosinophils synthesise TCA cycle intermediates

In addition to the generation of ATP and ROS, mitochondria can act as a biosynthetic hubs, synthesising TCA cycle intermediates and non-essential amino acids, however this has not been previously demonstrated in eosinophils. To test this, eosinophils were activated with IL-3, IL-5, or GM-CSF in the presence of $^{13}C_6$-glucose for 4 h. Upon activation, eosinophils incorperated ^{13}C-glucose into TCA cycle intermediates, such as citrate, succinate, malate and fumarate (Figure 3A-E). The metabolite pools analysed were mostly composed of the unlabelled (m+0) or m+2 mass isotopologue (Figure 3F; Supplementary Figure 1A-C) indicating lack of sustained TCA cycling.

Next, we determined whether TCA cycle intermediates are used as precursors for the synthesis of non-essential amino acids. Glutamate abundance was increased upon eosinophil stimulation with IL-3, IL-5 or GM-CSF (Figure 3G) and was largely present as the m+2 mass isotopologue (Figure 3H). While the eosinophils demonstrated production of glutamine and aspartate at baseline, cytokine stimulation had no further effect on the production of these. However, in comparison to the untreated control, cytokine-stimulated eosinophils had a reduced pool of ^{12}C unlabelled amino acids, indicating consumption of these amino acids (Supplementary Figure 2A-D).

Fully functional canonical TCA cycling requires two metabolite inputs: acetyl-CoA derived primarily from glucose and α-ketoglutarate derived from glutamine (Supplementary Figure 3A). Having established that eosinophils incorporate ^{13}C-glucose into TCA cycle intermediates, we next wanted to determine whether cytokine-activated eosinophils engage glutaminolysis. To address this, eosinophils were activated with IL-3, IL-5 or GM-CSF in the presence of ^{13}C-glutamine for 4 h. Incorporation of ^{13}C into TCA intermediates was increased in IL-3, IL-5 or GM-CSF treated eosinophils compared to the untreated controls (Supplementary Figure 3B).

The STAT5/PI3K/Akt axis governs the immediate metabolic response to IL-5

The development and clinical implementation of IL-5 targeting therapies in the treatment of asthma[31] prompted us to consider the early signalling mechanisms that govern increased ECAR

This article is protected by copyright. All rights reserved

and OCR in response to IL-5 treatment. STAT5 is activated upon IL-3, IL-5 or GM-CSF ligation[32,33], and in certain circumstances can be activated by ROS production via the common β chain[34]. We initially confirmed STAT5 phosphorylation in eosinophils treated with IL-3, IL-5 and GM-CSF. All cytokines induced STAT5 phosphorylation, but this only reached significance above baseline for IL-5 and GM-CSF (Figure 4A). Next, we wanted to determine whether inhibition of STAT5 affected the immediate ECAR and OCR responses of eosinophils treated with IL-5. Pre-treatment with the STAT5 inhibitor N′-((4-oxo-4H-chromen-3-yl)methylene)nicotinohydrazide (STAT5i) completely abrogated the ECAR and OCR response in IL-5-stimulated eosinophils (Figure 4B-C). Calculations of 'pre-cytokine' and 'post-cytokine' data can be found at Supplementary Figure 4.

In addition to cytokine-mediated STAT5 activation, both IL-5 and ROS can activate the PI3K/Akt axis[34], therefore we next investigated the role of PI3K/Akt in human eosinophil metabolism. Treatment with either the PI3K inhibitor LY294002 or the Akt1/2 inhibitor, abrogated IL-5 stimulated induction of ECAR (Figure 4D). The same trend was observed for OCR whereby the PI3K inhibitor reduced the immediate induction of OCR in eosinophils treated with IL-5 (Figure 4E). However, treatment with the Akt1/2 inhibitor did not reduce IL-5 induced OCR (Figure 4E), suggesting other downstream PI3K pathways may be involved. These data show that one of the key immediate effects of IL-5 on eosinophils is up-regulation of glycolysis and this is dependent on the STAT5/PI3K/Akt axis.

ROS inhibition reduces TCA cycling of IL-5 stimulated eosinophils

To determine if the observed cytokine-stimulated metabolic changes in eosinophils were promoted by ROS production we next determined whether NOX had a role in increased ECAR and OCR with a focus on IL-5 as before. Bioenergetic analyses were used to show that DPI had no effect on IL-5-stimulated glycolysis (Figure 5A) but significantly reduced peak OCR (Figure 5B). SITA using ^{13}C-glucose showed increased incorporation of ^{13}C into pyruvate and lactate (indicated as an increased m+3 mass isotopologue) in the presence of DPI (Figure 5C-D). This was accompanied by a reduction in the relative abundance of all TCA cycle intermediates (Figure 5E), represented by a decreased abundance of the m+2 mass isotopologue (Figure 5F). DPI treatment negatively impacted on the synthesis of amino acids glutamate and aspartate, from ^{13}C-glucose, by reducing ^{13}C incorporation and the m+2 mass isotopologue (Figure 5G-H). Collectively these data

This article is protected by copyright. All rights reserved

demonstrate that NOX-mediated ROS may have a critical role in driving mitochondrial metabolism.

Accepted Article

Discussion

This article is protected by copyright. All rights reserved

The study of eosinophil metabolism has been challenging, but recent years have seen the introduction of novel, refined technologies that allow metabolic analyses on low cell numbers with more sensitive readouts. This has been driven by the burgeoning field of immunometabolism and the increasingly recognised role of cellular metabolism in immune cell fate and function. Cellular metabolism through energy production (ATP) and biosynthetic intermediate generation orchestrates numerous effector roles such as cytokine production, migration and proliferation and can have a profound impact on various human pathologies[35]. Aside from their well-recognised energetic and biosynthetic roles, individual metabolites can have alternative roles. For example, TCA cycle metabolites, succinate and fumarate act as inflammatory signalling molecules. In LPS-stimulated macrophages, succinate stabilizes hypoxia-inducible factor-1α to promote increased glycolysis and IL-1β production[9,36,37]. Therefore, elucidating the cellular metabolic response of eosinophils not only improves our basic understanding of eosinophil function, especially how it might apply to tissue homeostasis, but has implications for revealing immunopathogenic and therapeutic strategies in eosinophilic disorders.

The rapid engagement of aerobic glycolysis by eosinophils in response to cytokines demonstrated here was accompanied by accumulation of both intra- and extracellular lactate. Lactate creates an acidic environment in which eosinophils are known to thrive, such as in the lung[38]. Furthermore, excess lactate retains T cells in pro-inflammatory environments, curtailing their migration[39]. If the same occurred for eosinophils this would provide a mechanism to retain viable eosinophils in an acidic inflammatory tissue environment. This increased glycolytic rate that supports the accumulation of lactate is presumably due to either GLUT1 or GLUT3 mediated glucose uptake as these transporters were expressed by all donors, or through kinetic effects on the direct phosphorylation of glycolytic enzymes[22].

A key feature of the work presented here is clarity surrounding the role of mitochondria in eosinophil metabolism. It is well established that eosinophils utilise their mitochondria for apoptotic purposes[10,30], however definitive metabolic contributions have remained elusive. Here, we confirmed that cytokine-stimulated eosinophils were sensitive to oligomycin treatment through a decrease in OCR. This indicates that mitochondria in eosinophils have an important role in mediating metabolic responses to cytokines which is in agreement with a previous study[5].

This article is protected by copyright. All rights reserved

Whilst the conversion of glucose to lactate seems to be the predominant metabolic pathway in response to cytokine stimulation, we used stable isotope tracing to show that eosinophils use both glucose and glutamine to generate TCA cycle intermediates and support OXPHOS upon activation. To our knowledge we are the first to provide evidence that carbons from glucose and glutamine are incorporated into TCA metabolites upon cytokine stimulation in eosinophils. Collectively, we reveal a novel role for human eosinophil mitochondria that extends beyond apoptosis and antibacterial defence. We demonstrate that eosinophils can utilise their mitochondria for TCA cycling contributions to OXPHOS and biosynthesis of amino acids. In support of a role for mitochondrial metabolism in eosinophils as we described here, a recent study indicated that peripheral blood eosinophils have increased oxidative parameters in comparison to neutrophils[5]. However, this interpretation was based solely on decreased oxygen consumption upon exposure to oligomycin and did not definitively characterise the metabolic fuels consumed by eosinophils.

The effects of IL-3, IL-5 and GM-CSF on eosinophil metabolism were broadly similar. To better understand the signalling processes that govern cytokine-mediated changes to eosinophil cellular metabolism we chose to focus on a single cytokine. IL-5 was chosen as it is a therapeutic target for treating eosinophilic asthma via monoclonal antibodies to IL-5 itself or IL-5Rα[31]. IL-5 ligation in human eosinophils has been shown to activate the JAK/STAT pathway, specifically STAT5[40,41]. With use of a specific STAT5 inhibitor we determined that increases in both ECAR and OCR upon IL-5 stimulation were dependent on STAT5 signalling. Because activated eosinophils increased their glucose utilization substantially, our attention turned to the PI3K/Akt axis as it is known to control glycolysis in other immune cell types such as T cells and macrophages[42,43]. PI3K and Akt inhibitors had a profound effect on the IL-5 mediated metabolic switch, especially glycolysis, showing that the IL-5 induced metabolic switch in human eosinophils is mediated by the STAT5/PI3K/Akt signalling axis. The IL-5 induced OCR was abrogated with PI3K inhibition but not Akt. This suggests that there are alternative downstream PI3K pathways contributing to increased oxygen consumption, such as the PI3K/Rac pathway[44]. Respiratory burst in eosinophils has been closely linked previously with the Rac pathway, thus offering a plausible explanation for our observations[15]. Elucidating roles of multiple Akt-independent downstream PI3K targets and their contributions to eosinophil metabolism warrants further investigation.

This article is protected by copyright. All rights reserved

Finally, we considered the link between ROS production and metabolic pathway activity in eosinophils again focussing on the effects of IL-5. Treatment of eosinophils with IL-5 has been shown to induce ROS production[23] and here we show that IL-5 increases oxygen consumption. As NOX-dependent respiratory burst is a fundamental effector function of eosinophils[14] we sought to investigate the role of ROS in eosinophil metabolism. Inhibiting NOX-dependent ROS production reduced the abundance of TCA cycle intermediates while increasing the accumulation of glucose-derived lactate suggesting that ROS may be a driver of eosinophil mitochondria metabolism in particular. This highlights that different bioactive molecules in the immediate microenvironment of eosinophils shape their metabolic plasticity.

Our study outlines the metabolic requirements of mitochondria in cytokine-activated eosinophils. We also show that ROS may enable metabolic plasticity. Taken together, this provides further insight into the mechanistic control of eosinophil function. It is likely that terminally differentiated cells such as eosinophils do not require extensive energy production and biosynthesis to support homeostasis or activation. Instead multiple cytokines and important mediators such as eosinophil-derived neurotoxins and peroxidases are contained within pre-formed granules. However, cytokine-mediated activation clearly up-regulates cytoplasmic and mitochondrial metabolic pathways. This raises further questions about the links between eosinophil function and metabolism including the bioenergetic demands of piecemeal degranulation and the effects of mitochondrial DNA release on the metabolic status of eosinophils. Eosinophils are a characteristic feature of type 2 immune responses linked to immunopathology in asthma and other inflammatory disorders but also to tissue defence and repair processes in helminthic parasite infection[45] and in other settings including metabolic homeostasis in adipose tissue[6]. Greater understanding of the regulation of eosinophil recruitment, retention and survival would provide mechanistic insight and offer new metabolically targeted therapeutic approaches for respiratory and other eosinophilic diseases. Cell-specific delivery systems of pharmacological agents via for example Siglec-8 could be one route[46] or more general approaches to limiting lactate in the tissue microenvironment during pathology might have broad effects on multiple cells types[39], including eosinophils.

This article is protected by copyright. All rights reserved

Accepted Article

Acknowledgments

We thank D. Avizonis and L. Choinière from McGill University Metabolomics Core Facility, C. Von Ruhland from Central Biotechnology Services Cardiff, D. Morgan, T. DeCoursey and C. Mauro for useful discussion, A. Tonks for laboratory assistance, staff in the Joint Clinical Research Facility for phlebotomy and all blood donors. This work was supported with grants awarded by Life Sciences Research Network Wales (NRN), and the Natural Sciences and

This article is protected by copyright. All rights reserved

Engineering Research Council (NSERC) in Canada. EEV was supported by CRUK (C18281/A19169) and is now supported by a Diabetes UK RD Lawrence Fellowship (17/0005587). L.C.F. was supported by a Postdoctoral Fellowship from NSERC. Flow Cytometry for ROS measurements was performed at the University of Alberta, Faculty of Medicine and Dentistry Flow Cytometry Facility, which received financial support from the Faculty of Medicine and Dentistry and the Canada Foundation for Innovation (CFI) awards to contributing investigators.

Authorship Contributions

NJ, EEV, LCF, JGC, LMS performed the experiments; PSH, PL and CAT provided intellectual discussion. NJ, EEV, PSH, PL and CAT designed the experiments. NJ, EEV, PL and CAT wrote the manuscript. All authors critically revised and approved the manuscript.

Conflicts of Interest

The authors declare no conflicts of interest.

References

1. Kim JD, Willetts L, Ochkur S, et al. An essential role for Rab27a GTPase in eosinophil exocytosis. *J Leukoc Biol.* 2013;94(6):1265-1274.
2. Fulkerson PC, Rothenberg ME. Targeting eosinophils in allergy, inflammation and beyond. *Nat Rev Drug Discov.* 2013;12(2):117-129.

This article is protected by copyright. All rights reserved

Accepted Article

Accepted Article

3. Rosenberg HF, Dyer KD, Foster PS. Eosinophils: changing perspectives in health and disease. *Nat Rev Immunol.* 2013;13(1):9-22.
4. Wenzel SE. Asthma phenotypes: the evolution from clinical to molecular approaches. *Nat Med.* 2012;18(5):716-725.
5. Porter L, Toepfner N, Bashant KR, et al. Metabolic Profiling of Human Eosinophils. *Front Immunol.* 2018;9:1404.
6. Wu D, Molofsky AB, Liang HE, et al. Eosinophils sustain adipose alternatively activated macrophages associated with glucose homeostasis. *Science.* 2011;332(6026):243-247.
7. Sadiku P, Willson JA, Dickinson RS, et al. Prolyl hydroxylase 2 inactivation enhances glycogen storage and promotes excessive neutrophilic responses. *J Clin Invest.* 2017;127(9):3407-3420.
8. Sumbayev VV, Yasinska I, Oniku AE, Streatfield CL, Gibbs BF. Involvement of hypoxia-inducible factor-1 in the inflammatory responses of human LAD2 mast cells and basophils. *PLoS One.* 2012;7(3):e34259.
9. Jones R, McDonald KE, Willson JA, et al. Mutations in succinate dehydrogenase B (SDHB) enhance neutrophil survival independent of HIF-1alpha expression. *Blood.* 2016;127(21):2641-2644.
10. Peachman KK, Lyles DS, Bass DA. Mitochondria in eosinophils: functional role in apoptosis but not respiration. *Proc Natl Acad Sci U S A.* 2001;98(4):1717-1722.
11. Yousefi S, Gold JA, Andina N, et al. Catapult-like release of mitochondrial DNA by eosinophils contributes to antibacterial defense. *Nat Med.* 2008;14(9):949-953.
12. Mukherjee M, Lacy P, Ueki S. Eosinophil Extracellular Traps and Inflammatory Pathologies-Untangling the Web! *Front Immunol.* 2018;9:2763.
13. Kovacs I, Horvath M, Kovacs T, et al. Comparison of proton channel, phagocyte oxidase, and respiratory burst levels between human eosinophil and neutrophil granulocytes. *Free Radic Res.* 2014;48(10):1190-1199.
14. Gaurav R, Bewtra AK, Agrawal DK. Chloride Channel 3 Channels in the Activation and Migration of Human Blood Eosinophils in Allergic Asthma. *Am J Respir Cell Mol Biol.* 2015;53(2):235-245.

This article is protected by copyright. All rights reserved

Accepted Article

15. Lacy P, Abdel-Latif D, Steward M, Musat-Marcu S, Man SF, Moqbel R. Divergence of mechanisms regulating respiratory burst in blood and sputum eosinophils and neutrophils from atopic subjects. *J Immunol.* 2003;170(5):2670-2679.
16. Rafalski VA, Mancini E, Brunet A. Energy metabolism and energy-sensing pathways in mammalian embryonic and adult stem cell fate. *J Cell Sci.* 2012;125(Pt 23):5597-5608.
17. Yoshida T, Shevkoplyas SS. Anaerobic storage of red blood cells. *Blood Transfus.* 2010;8(4):220-236.
18. Rodriguez-Espinosa O, Rojas-Espinosa O, Moreno-Altamirano MM, Lopez-Villegas EO, Sanchez-Garcia FJ. Metabolic requirements for neutrophil extracellular traps formation. *Immunology.* 2015;145(2):213-224.
19. Menk AV, Scharping NE, Moreci RS, et al. Early TCR Signaling Induces Rapid Aerobic Glycolysis Enabling Distinct Acute T Cell Effector Functions. *Cell Rep.* 2018;22(6):1509-1521.
20. Phong B, Avery L, Menk AV, Delgoffe GM, Kane LP. Cutting Edge: Murine Mast Cells Rapidly Modulate Metabolic Pathways Essential for Distinct Effector Functions. *J Immunol.* 2017;198(2):640-644.
21. David JR, Butterworth AE, Remold HG, David PH, Houba V, Sturrock RF. Antibody-dependent, eosinophil-mediated damage to 51Cr-labeled schistosomula of Schistosoma mansoni: effect of metabolic inhibitors and other agents which alter cell function. *J Immunol.* 1977;118(6):2221-2229.
22. Venge P, Moberg L, Bjornsson E, Bergstrom M, Langstrom B, Hakansson L. Mechanisms of basal and cytokine-induced uptake of glucose in normal human eosinophils: relation to apoptosis. *Respir Med.* 2003;97(10):1109-1119.
23. Horie S, Gleich GJ, Kita H. Cytokines directly induce degranulation and superoxide production from human eosinophils. *J Allergy Clin Immunol.* 1996;98(2):371-381.
24. Esnault S, Kelly EA, Shen ZJ, Johansson MW, Malter JS, Jarjour NN. IL-3 Maintains Activation of the p90S6K/RPS6 Pathway and Increases Translation in Human Eosinophils. *J Immunol.* 2015;195(6):2529-2539.
25. Gregory B, Kirchem A, Phipps S, et al. Differential regulation of human eosinophil IL-3, IL-5, and GM-CSF receptor alpha-chain expression by cytokines: IL-3, IL-5, and GM-

This article is protected by copyright. All rights reserved

CSF down-regulate IL-5 receptor alpha expression with loss of IL-5 responsiveness, but up-regulate IL-3 receptor alpha expression. *J Immunol.* 2003;170(11):5359-5366.
26. Demaurex N, El Chemaly A. Physiological roles of voltage-gated proton channels in leukocytes. *J Physiol.* 2010;588(Pt 23):4659-4665.
27. Bankers-Fulbright JL, Kephart GM, Bartemes KR, Kita H, O'Grady SM. Platelet-activating factor stimulates cytoplasmic alkalinization and granule acidification in human eosinophils. *J Cell Sci.* 2004;117(Pt 24):5749-5757.
28. Mookerjee SA, Goncalves RLS, Gerencser AA, Nicholls DG, Brand MD. The contributions of respiration and glycolysis to extracellular acid production. *Biochim Biophys Acta.* 2015;1847(2):171-181.
29. Pearce EL, Pearce EJ. Metabolic pathways in immune cell activation and quiescence. *Immunity.* 2013;38(4):633-643.
30. Ilmarinen P, Moilanen E, Kankaanranta H. Mitochondria in the center of human eosinophil apoptosis and survival. *Int J Mol Sci.* 2014;15(3):3952-3969.
31. Farne HA, Wilson A, Powell C, Bax L, Milan SJ. Anti-IL5 therapies for asthma. *Cochrane Database Syst Rev.* 2017;9:CD010834.
32. Wingelhofer B, Neubauer HA, Valent P, et al. Implications of STAT3 and STAT5 signaling on gene regulation and chromatin remodeling in hematopoietic cancer. *Leukemia.* 2018.
33. Kano G, Almanan M, Bochner BS, Zimmermann N. Mechanism of Siglec-8-mediated cell death in IL-5-activated eosinophils: role for reactive oxygen species-enhanced MEK/ERK activation. *J Allergy Clin Immunol.* 2013;132(2):437-445.
34. Chen S, Su Y, Wang J. ROS-mediated platelet generation: a microenvironment-dependent manner for megakaryocyte proliferation, differentiation, and maturation. *Cell Death Dis.* 2013;4:e722.
35. Mathis D, Shoelson SE. Immunometabolism: an emerging frontier. *Nat Rev Immunol.* 2011;11(2):81.
36. Del Rey MJ, Valin A, Usategui A, et al. Hif-1alpha Knockdown Reduces Glycolytic Metabolism and Induces Cell Death of Human Synovial Fibroblasts Under Normoxic Conditions. *Sci Rep.* 2017;7(1):3644.

Accepted Article

This article is protected by copyright. All rights reserved

37. Tannahill GM, Curtis AM, Adamik J, et al. Succinate is an inflammatory signal that induces IL-1beta through HIF-1alpha. *Nature.* 2013;496(7444):238-242.
38. Kottyan LC, Collier AR, Cao KH, et al. Eosinophil viability is increased by acidic pH in a cAMP- and GPR65-dependent manner. *Blood.* 2009;114(13):2774-2782.
39. Haas R, Smith J, Rocher-Ros V, et al. Lactate Regulates Metabolic and Pro-inflammatory Circuits in Control of T Cell Migration and Effector Functions. *PLoS Biol.* 2015;13(7):e1002202.
40. Caldenhoven E, van Dijk TB, Tijmensen A, et al. Differential activation of functionally distinct STAT5 proteins by IL-5 and GM-CSF during eosinophil and neutrophil differentiation from human CD34+ hematopoietic stem cells. *Stem Cells.* 1998;16(6):397-403.
41. Stout BA, Bates ME, Liu LY, Farrington NN, Bertics PJ. IL-5 and granulocyte-macrophage colony-stimulating factor activate STAT3 and STAT5 and promote Pim-1 and cyclin D3 protein expression in human eosinophils. *J Immunol.* 2004;173(10):6409-6417.
42. Gubser PM, Bantug GR, Razik L, et al. Rapid effector function of memory CD8+ T cells requires an immediate-early glycolytic switch. *Nat Immunol.* 2013;14(10):1064-1072.
43. Covarrubias AJ, Aksoylar HI, Horng T. Control of macrophage metabolism and activation by mTOR and Akt signaling. *Semin Immunol.* 2015;27(4):286-296.
44. Lien EC, Dibble CC, Toker A. PI3K signaling in cancer: beyond AKT. *Curr Opin Cell Biol.* 2017;45:62-71.
45. Lloyd CM, Snelgrove RJ. Type 2 immunity: Expanding our view. *Sci Immunol.* 2018;3(25).
46. Kiwamoto T, Kawasaki N, Paulson JC, Bochner BS. Siglec-8 as a drugable target to treat eosinophil and mast cell-associated conditions. *Pharmacol Ther.* 2012;135(3):327-336.

Accepted Article

This article is protected by copyright. All rights reserved

Figure Legends

Figure 1. IL-3, IL-5 or GM-CSF stimulated eosinophils increase glycolytic metabolism and production of lactate. (A) Expression levels of glucose transporters *(GLUT) 1-4*. (B) Representative flow cytometry plot of glucose uptake by eosinophils activated for 1 h with IL-3, IL-5 or GM-CSF (10 ng/mL) using probe 2-(*N*-(7-nitrobenz-2-oxa-1,3-diazol-4-yl)amino)-2-deoxyglucose (2-NBDG; 100 μM). (C) Glycolytic stress profile of eosinophils by measuring extracellular acidification rate (ECAR; mpH/min) before and following addition of IL-3, IL-5, GM-CSF (10 ng/mL), glucose (5.5 mM), oligomycin (1 μM) and 2-DG (100 mM) at the time points indicated. (D) Post-glucose ECAR calculated via the averaged ECAR values from measurement points 7-9 minus the averaged ECAR values from measurement points 1-3. (E) Schematic of uniformly labelled $^{13}C_6$-glucose incorporation into pyruvate and lactate. Eosinophils were activated with IL-3, IL-5, or GM-CSF (10 ng/mL) for 4 h. (F) Relative abundance of ^{12}C and ^{13}C pyruvate. (G) Mass isotopologue distribution (MID) of the pyruvate pool. (H) Relative abundance of ^{12}C and ^{13}C lactate including (I) MID of the lactate pool. (J) Relative abundance of ^{12}C and ^{13}C extracellular lactate. (K) Extracellular lactate production of eosinophils treated with IL-3, IL-5 or GM-CSF (10 ng/mL) for 4 h. Data are represented as mean ± SEM of 7 (A), 4 (B), 3-5 (C-D, F-I), 2-3 (J) and 2-4 (K) independent experiments with each data point representing an individual donor. Statistical analysis was performed using a one-way ANOVA with multiple comparisons to the control group (D, K) or a two-way ANOVA (F-J); * $p \leq 0.05$, ** $p \leq 0.01$, *** $p \leq 0.001$.

Figure 2. Cytokine treatment induces mitochondrial-independent ROS production (A) Mitochondrial morphology of human eosinophils by TEM. (B) Oxidative stress assay measured via oxygen consumption rate (OCR; pmoles/min) before and following addition of IL-3, IL-5, GM-CSF (10 ng/mL), glucose (5.5 mM), oligomycin (1 μM) and 2-DG (100 mM) at the time points indicated. (C) Percentage OCR increase in comparison to baseline. (D) Glycolytic stress and (E) oxidative stress IL-3 dose response. Eosinophils were given IL-3 (10, 50 and 100 ng/mL), glucose (5.5 mM), oligomycin (1 μM) and 2-DG (100 mM) at the time points indicated. (F) Representative flow cytometry plot and (G) MitoSOX^{+ve} population of eosinophils activated with IL-3, IL-5 or GM-CSF (10 ng/mL) and incubated with MitoSOX for 15 min. (H) Representative flow cytometry plots of total intracellular ROS production measured by CellROX from one donor and (I) CellROX^{+ive} population of eosinophils stimulated with IL-3, IL-5 or GM-CSF (10 ng/mL)

This article is protected by copyright. All rights reserved

± DPI (10 μM). Dotted line indicates unstimulated controls in the presence of CellROX. Data expressed as mean ± SEM of 2 (A), 3-5 (B-C), 2 (D-E), 4-5 (G) and 6-8 (I) independent experiments with each data point representing an individual donor. Statistical analysis was performed using a one-way ANOVA with multiple comparisons to the control group (C) or an unpaired t test (I); * $p \leq 0.05$, *** $p \leq 0.001$.

Figure 3. IL-3, IL-5 or GM-CSF treatment induces the production of TCA cycle intermediates. (A) Schematic of uniformly labelled $^{13}C_6$-glucose incorporation into TCA cycle intermediates. Eosinophils were activated with IL-3, IL-5 or GM-CSF (10 ng/mL) for 4 h. Relative abundance of ^{12}C and ^{13}C (B) citrate, (C) succinate, (D) malate and (E) fumarate. (F) Mass isotopologue distribution (MID) of m+2 citrate, succinate and malate. (G) Relative abundance of ^{12}C and ^{13}C glutamate including the (H) MID distribution. All data are from 3-6 independent experiments with each data point representing an individual donor. Data expressed as mean ± SEM. Statistical analysis was performed using a two-way ANOVA; * $p \leq 0.05$, ** $p \leq 0.01$, *** $p \leq 0.001$.

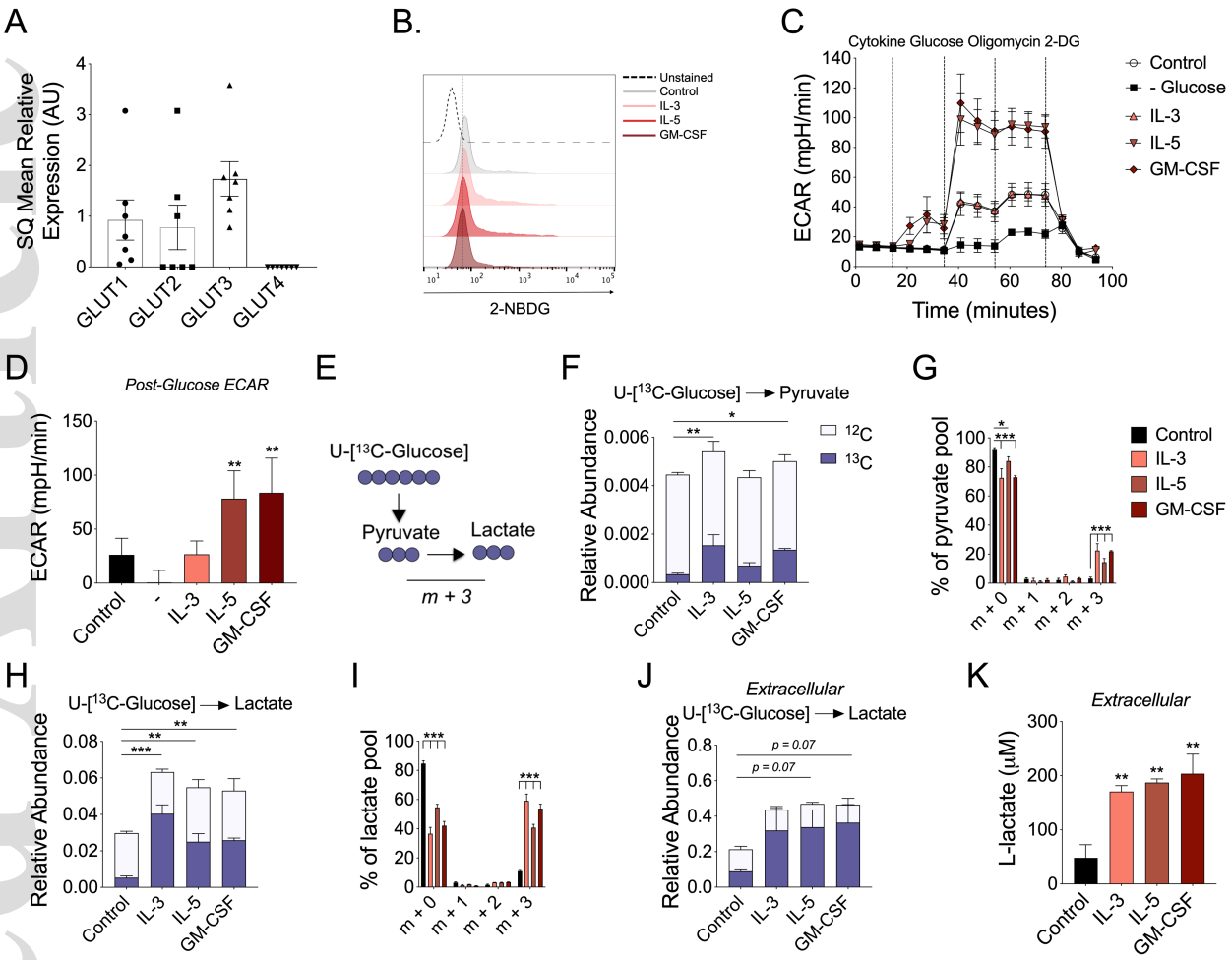
Figure 4. The STAT5/PI3K/Akt axis is responsible for the metabolic switch in IL-5 treated eosinophils. (A) Representative immunoblot of eosinophils treated for 15 min with IL-3, IL-5 or GM-CSF (10 ng/mL) for $pSTAT5^{694}$ and β-actin. Corresponding densitometry analysis of pSTAT5 normalised to β-actin. (B) ECAR and (C) OCR before and following addition of a STAT5 inhibitor (STAT5i; N′-((4-oxo-4H-chromen-3-yl)methylene)nicotinohydrazide; 100 μM), IL-5 (10 ng/mL) and 2-DG (100 mM), including 'pre-cytokine' activation and 'post-cytokine' activation pooled OCR and ECAR data. (D) ECAR and (E) OCR before and following addition of a PI3K inhibitor (LY294002; 10 μM) or Akt1/2 inhibitor (1,3-dihydro-1-(1-((4-(6-phenyl-1H-imidazo[4,5-g]quinoxalin-7-yl)phenyl)methyl)-4-piperidinyl)-2H-benzimidazol-2-one trifluoroacetate salt hydrate; 10 μM), IL-5 (10 ng/mL) and 2-DG (100 mM). Data expressed as mean ± SEM of 5 (A), 2-3 (B-C) and 4 (D-E) independent experiments with each data point representing an individual donor. Statistical analysis was performed using a Friedman test with Dunn's multiple comparisons (A) or a two-way ANOVA with Sidak's multiple comparison test (B-E); * $p \leq 0.05$, ** $\leq p$ 0.01, *** $p \leq 0.001$.

This article is protected by copyright. All rights reserved

Figure 5. DPI inhibits oxidative metabolism in IL-5 stimulated eosinophils. (A) ECAR (mpH/min) and (B) OCR (pmoles/min) of eosinophils treated with IL-5 (10 ng/mL) ± DPI (100 nM), glucose (5.5 mM), oligomycin (1 μM) and 2-DG (100 mM). Eosinophils were activated with IL-5 (10 ng/mL) ± DPI (100 nM) for 4 h in the presence of ^{13}C-glucose. (C) Relative abundance of ^{12}C and ^{13}C and (D) mass isotopologue distribution (MID) of glycolytic intermediates pyruvate and lactate. (E) Relative abundance of ^{12}C and ^{13}C and (F) MID of TCA cycle intermediates citrate, succinate, fumarate and malate. (G) Relative abundance of ^{12}C and ^{13}C and (H) MID of amino acids glutamate and aspartate. Data expressed as mean ± SEM of 4 (A-B) and 3 (C-H) independent experiments with each data point representing an individual donor. Statistical analysis was performed using an unpaired t test (B) or a two way ANOVA (C-H); * $p \leq 0.05$, ** $\leq$ p 0.01, *** $p \leq 0.001$.

Accepted Article

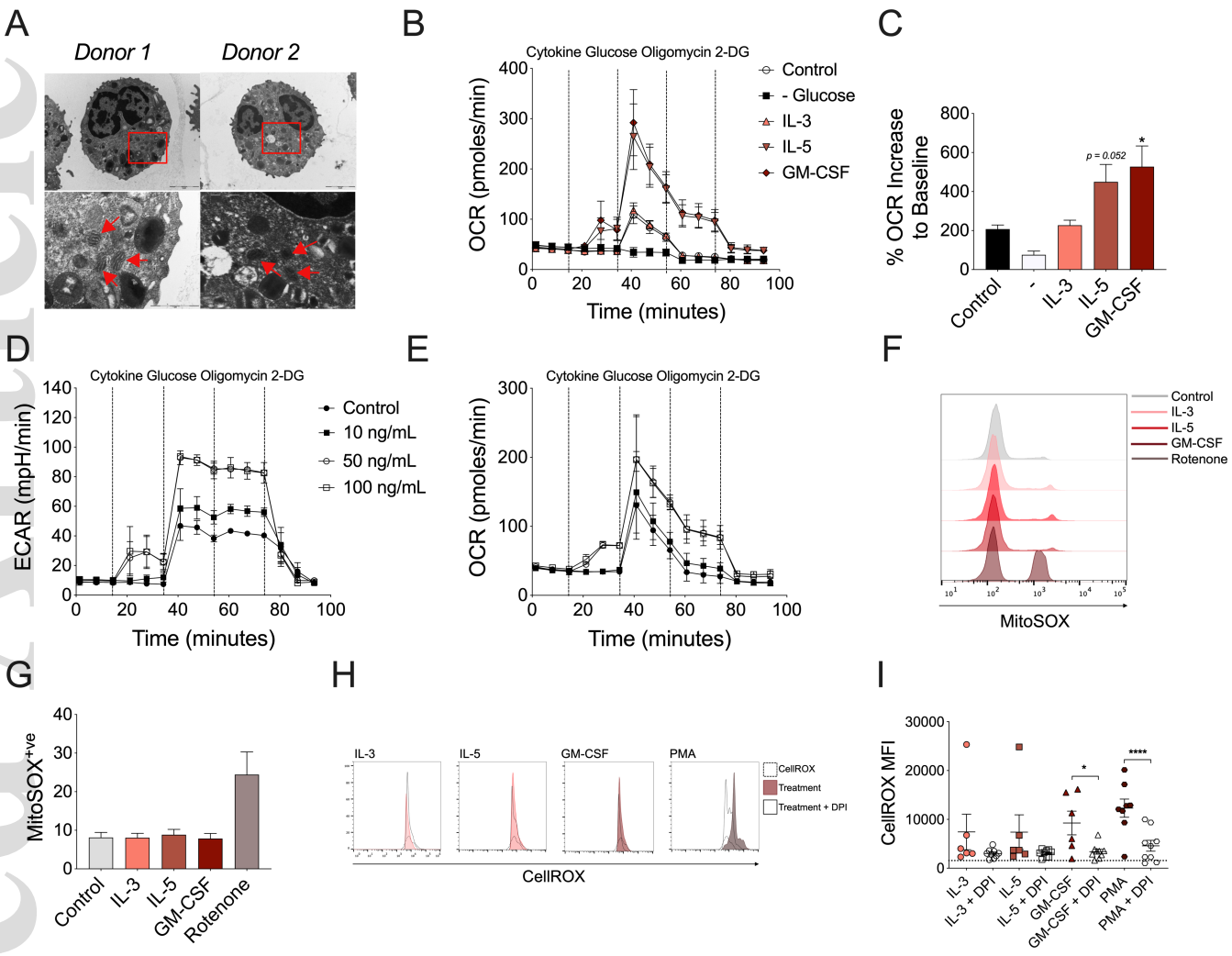
This article is protected by copyright. All rights reserved



all_14158_f1.tiff

This article is protected by copyright. All rights reserved

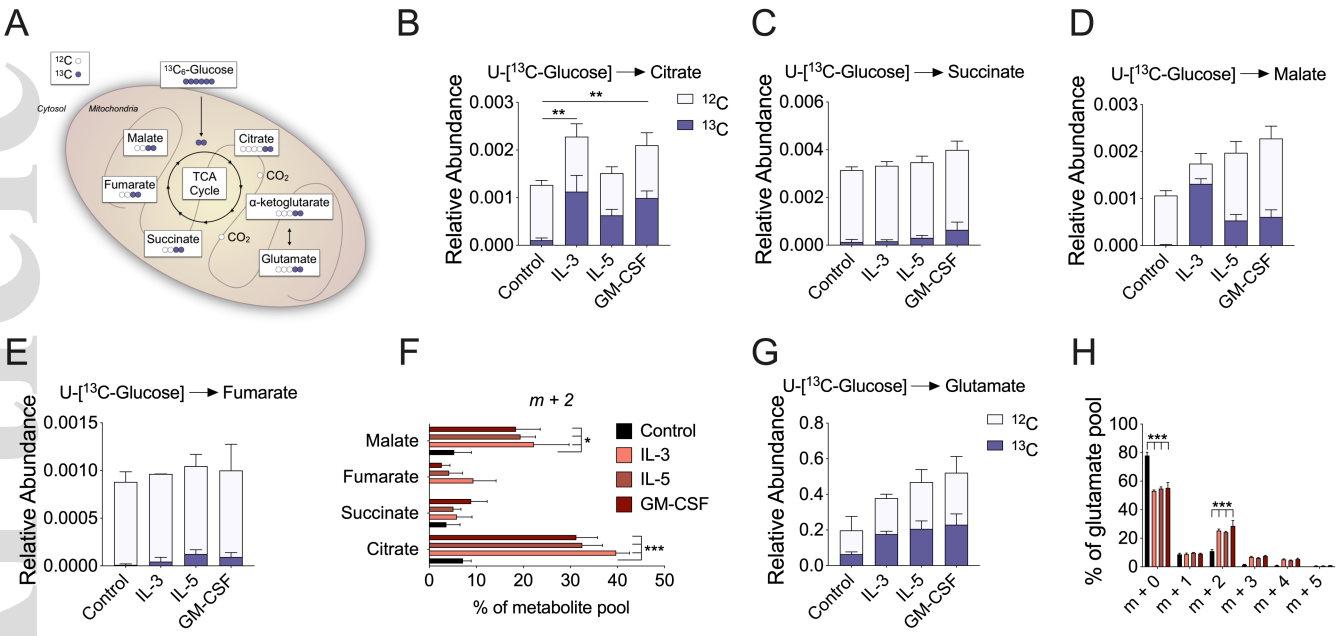
Accepted Article



all_14158_f2.tiff

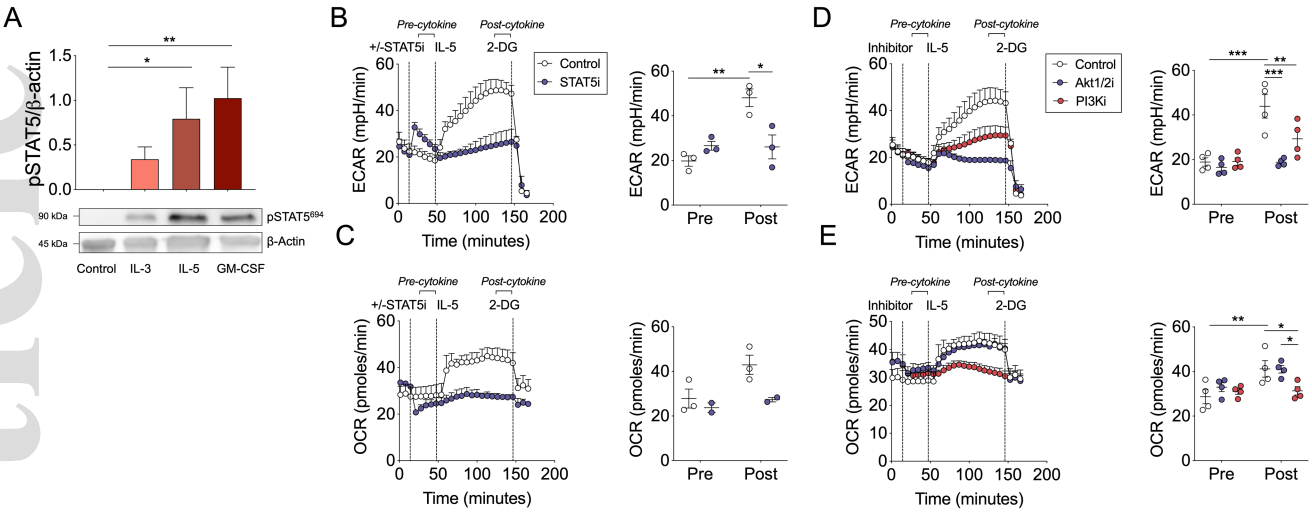
This article is protected by copyright. All rights reserved

Accepted Article



all_14158_f3.tiff

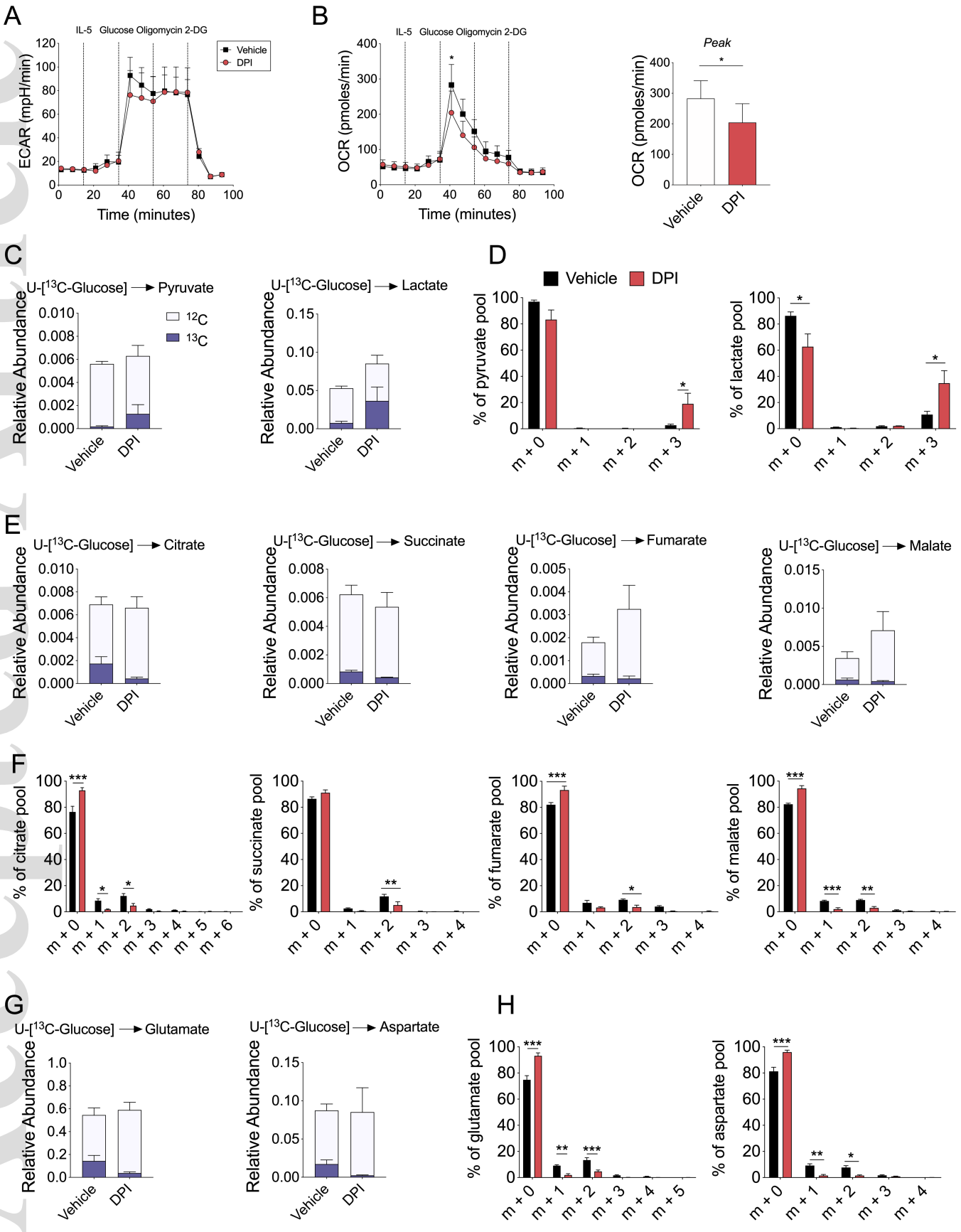
This article is protected by copyright. All rights reserved



all_14158_f4.tiff

Accepted Article

This article is protected by copyright. All rights reserved



all_14158_f5.tiff

This article is protected by copyright. All rights reserved

Online Supplement

Title: Interleukin-5 drives glycolysis and reactive oxygen species-dependent citric acid cycling by eosinophils

Authors: Nicholas Jones[1], Emma E. Vincent [2,3], Lindsey C. Felix[4], James G. Cronin[1], Louis M. Scott[1], Paul S. Hole[5], Paige Lacy[4] and Catherine A. Thornton[1,*]

Affiliations: [1]Institute of Life Science, Swansea University Medical School, Swansea, SA2 8PP, United Kingdom. [2]MRC Integrative Epidemiology Unit, University of Bristol, Oakfield House, Bristol, BS8 2BN, United Kingdom. [3]Cellular and Molecular Medicine, University of Bristol, Biomedical Sciences Building, Bristol, BS8 1TD, United Kingdom. [4]Alberta Respiratory Centre (ARC), Department of Medicine, University of Alberta, Edmonton, Alberta, T6G 2G3 Canada. [5]Department of Haematology, Division of Cancer and Genetics, School of Medicine, Cardiff University, Cardiff, CF14 4XN, United Kingdom.

[*] Corresponding author: Professor Cathy Thornton
Swansea University Medical School
Singleton Park
Swansea
SA2 8PP
E-mail: c.a.thornton@swansea.ac.uk
Telephone: +44 (0) 1792 602122.

Materials and Methods

Human eosinophil isolation

Human peripheral blood was collected from both male (n = 9) and female donors (n = 25) aged between 18-70 years into heparinised Vacuettes^{TM} (Greiner Bio-one, Frickenhausen, Germany). We recruited both atopic and non-atopic donors with eosinophils comprising between 1-8% of total circulating leukocytes. Specific donor demographics can be found in supplementary table 1. All samples were collected with informed written consent and ethical approval was obtained from Wales Research Ethics Committee 6 (13/WA/0190). Polymorphonuclear cells were isolated by layering whole blood (1:1) onto histopaque (Sigma-Aldrich, Poole, UK) prior to centrifugation at 805 x *g* for 20 min at room temperature. The erythrocyte pellet was lysed with hypotonic buffer (0.8% NH_4Cl, 10 mM $NaHCO_3$ and 0.1 mM EDTA (Sigma-Aldrich, UK)) for 10 min with gentle agitation. Eosinophils were isolated by negative selection using immunomagnetic microbeads (autoMACS; Miltenyi Biotec, Cologne, Germany). The percentage purity for isolated eosinophil populations was consistently >95%. For ROS measurements, eosinophils were isolated using a similar kit (MACSxpress) as described by the manufacturer (Miltenyi Biotec), with similar purity and viability[1].

Flow cytometry

Purity of eosinophils was monitored using flow cytometry. Briefly, 1.0 x 10^5 cells were left unstained or incubated with anti-CCR3 VioBlue (CD193, IgG1, REA574) or anti-Siglec8 PE (IgG1κ, 7C9) using standard techniques.

For glucose uptake, eosinophils were stimulated with recombinant human IL-3, IL-5 and GM-CSF (10 ng/mL; Miltenyi Biotec) for 1 h in glucose-free RPMI and 2-(*N*-(7-nitrobenz-2-oxa-1,3-diazol-4-yl)amino)-2-deoxyglucose (2-NBDG; 100 μM) was added for 10 min. Cells were then washed twice, acquired on a flow cytometer (Novocyte, ACEA) and downstream analysis was performed using FlowJo version 10 (Tree Star, Oregon, USA).

Quantitative real time PCR

RNA was extracted using the RNeasy Mini Kit and automated Qiacube system, according to the manufacturer's instructions (Qiagen, Crawley, UK). Extracted RNA was quantified (Nanodrop ND1000 spectrophotometer, Labtech, Ringmer, UK). For

cDNA synthesis, 1 µg of total RNA was added to a genomic DNA elimination reaction, followed by conversion to cDNA (Quantitect Reverse Transcription Kit, Qiagen), according to the manufacturer's instructions. Gene expression by qPCR was with intron-spanning gene-specific primers (Supplementary Table 2) and the IQ5 system (Bio-Rad, Hemel Hempstead, UK). The starting quantity of mRNA from experimental samples was determined using standard curves generated from reference cDNA (Quantifast SYBR green, Qiagen). mRNA expression levels were normalized to house-keeping genes 18S and RPL19. All PCR analyses were conducted in triplicate.

Extracellular flux analysis

Metabolic analyses were carried out using a Seahorse XF^{e}96 Analyzer (Agilent). Briefly, 1.5 x 10^5 cells were seeded onto a Cell-Tak (Corning) coated microplate.

Short-term activation: Glycolytic and oxidative stress were measured simultaneously via extracellular acidification rates (ECAR; mpH/min) and oxygen consumption rates (OCR; pmoles/min), respectively. Eosinophils were resuspended in XF assay media supplemented with 2 mM glutamine and addition of media control or IL-3, IL-5 or GM-CSF (all 10 ng/mL; all Miltenyi Biotec), glucose (5.5 mM), oligomycin (1 µM) and 2-deoxy-D-glucose (100 mM; all chemicals were purchased from Sigma) were used. For ROS inhibition experiments, diphenyleneiodonium chloride (DPI; 100 nM) was combined with IL-5 (10 ng/mL).

Long-term activation: Eosinophils were resuspended in XF Assay media supplemented with 5.5 mM glucose and 2 mM glutamine. Baseline ECAR and OCR were determined for 3 cycles prior to the addition of STAT5 inhibitor N′-((4-oxo-4H-chromen-3-yl)methylene)nicotinohydrazide (100 µM; Merck), PI3K inhibitor, LY294002 (10 µM; Calbiochem) or Akt1/2 inhibitor (10 µM; Sigma-Aldrich). A 30 min period of incubation with the inhibitor occurred prior to the addition of IL-5 (10 ng/mL). Corresponding ECAR was monitored for 1.5 h after cytokine/vehicle introduction. A final addition of 2-DG (100 mM) arrested glycolysis.

Stable isotope tracer analysis and GC-MS

Isolated eosinophils were incubated with universally heavy labelled ^{13}C glucose (11.1 mM; Cambridge Isotopes) in glucose free RPMI (ThermoFisher Scientific) or ^{13}C glutamine (2 mM; Cambridge Isotopes) in glutamine free RPMI (ThermoFisher

Scientific) with 10% dialyzed FBS (ThermoFisher Scientific). Eosinophils were activated with IL-3, IL-5 or GM-CSF (10 ng/mL) for a period of 4 h. For ROS inhibition, ^{13}C glucose cultured eosinophils were activated with IL-5 (10 ng/mL) in the presence or absence of DPI (100 nM). Cells were then washed twice with ice cold PBS and lysed in 80% methanol. Cell supernatant (10 µL) was harvested and added to 80% methanol. Cell extracts and supernatant were then dried down at 4°C using a speed-vacuum concentrator.

Cellular metabolites were extracted and analyzed by gas chromatography-mass spectrometry (GC-MS) using protocols described previously[2,3]. Briefly, metabolite extracts were derived using N-(*tert*-butyldimethylsilyl)-N-methyltrifluoroacetamide (MTBSTFA). D-myristic acid (750 ng/sample) was added as an internal standard to metabolite extracts, and metabolite abundance was expressed relative to the internal standard. GC/MS analysis was performed using an Agilent 5975C GC/MS equipped with a DB-5MS+DG (30 m x 250 µm x 0.25 µm) capillary column (Agilent J&W, Santa Clara, CA, USA). For SITA experiments, mass isotopomer distribution was determined using a custom algorithm developed at McGill University[2].

Extracellular lactate measurement

Extracellular lactate was measured using the L-lactate assay kit I (Eton Bioscience) as per manufacturer's instructions.

Transmission electron microscopy

Eosinophils were fixed in 1% glutaraldehyde in 10 mM PBS for 1 h and stored in PBS at 4°C. Fixed cells were pre-immobilized in agar by centrifuging at 500 x *g* for 5 min and mixing the resulting pellet 1:1 with 4% molten low melting point agar at 50°C and allowing to cool. The resulting block was post-fixed in 1% osmium tetroxide for 2 h, thoroughly washed, dehydrated through graded propan-2-ol (50, 70, 90 and 100% for 15 min each), infiltrated for 30 min in 50% TAAB embedding resin (TER) (TAAB Laboratories Equipment Ltd. UK) in propan-2-ol, and 3 x 1 h in 100% TER before being embedded in 100% TER at 60°C for 24 h. 80 nm thick sections were collected onto 300 mesh copper grids and stained with uranyl acetate and lead citrate. Samples were examined in a Philips CM12 TEM (FEI U. K. Ltd. UK) at 80 kV and images captured with a Megaview III camera and AnalySIS software (Soft

Imaging System GmbH, Germany).

ROS detection

Mitochondria-derived superoxide production was measured using MitoSOX Red (Thermo Fisher Scientific). Briefly, 0.25 x 10^6 cells were incubated with IL-3, IL-5 or GM-CSF (all 10 ng/mL), MitoSOX (5 μM) and DRAQ7 (1 μM; Biostatus, UK) for 15 min at 37 °C in 5% CO_2-in-air. Rotenone was used as a positive control (50 μM). Cells were analysed by flow cytometry as before.

For total ROS, eosinophils (1 × 10^6 cells/mL) were rested on ice for 1 h in RPMI 1640 medium (Life Technologies) supplemented with 25 mM HEPES, 2 mM L-glutamine, and 0.1% fraction V BSA (Sigma-Aldrich). Eosinophils were treated with CellROX (5 μM; Life Technologies) ± cytokines (IL-3, IL-5 or GM-CSF; all 10 ng/mL) or the positive control (phorbol 12-myristate 13-acetate 61.7 ng/mL; Sigma-Aldrich) in the presence or absence of ROS inhibitor DPI (10 μM; Merck). Cells were incubated for 30 min at 37 °C in the dark with subsequent addition of agonists for 15 min. Cells were centrifuged at 300 x *g* for 5 min at 4 °C, washed with PBS (Life Technologies), and fixed with 4% paraformaldehyde (Electron Microscopy Sciences). Cells were acquired using a bench top digital flow cytometer (Attune NxT Acoustic Focusing Cytometer, Life Technologies).

Immunoblotting

Eosinophils were cultured at 1 x 10^6 cells/mL with IL-3, IL-5 or GM-CSF (10 ng/mL) for 15 min in RPMI supplemented with 10% fetal bovine serum (ThermoFisher Scientific). Protein levels were quantified and then separated using SDS-polyacrylamide gel electrophoresis and transfered to polyvinylidene membrane as described previously[4]. Membranes were probed with antibodies targeting phospho-STAT5 Tyr694 (9351; Cell Signaling Technology). Protein loading was evaluated and normalized using β-actin (3700; Cell Signaling Technology). Densitometry on non-saturated immunoblots was measured using ImageJ software (Fiji, ImageJ; NIH).

Data Analysis

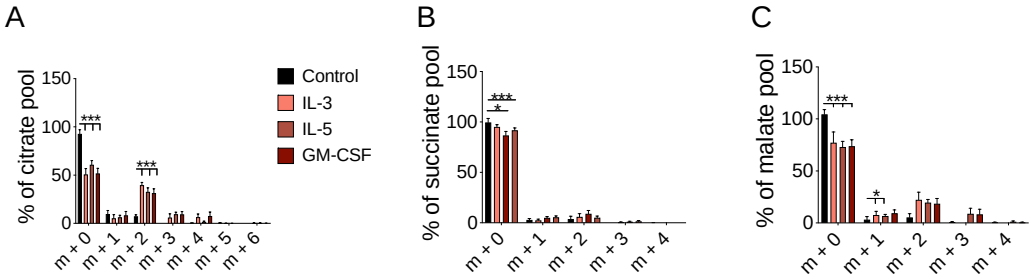
Statistical analysis was performed using GraphPad Prism version 8 (USA). Data are represented as the mean ± or + standard error of the mean (SEM). Significant values were taken as * $p \leq 0.05$, ** $p \leq 0.01$, *** $p \leq 0.001$.

Sex	Age	BMI	Medication
Female	55	22.405877	Asthma Inhaler
Male	32	38.3698743	Citalopram
Male	32	23.126619	
Female	32	36.2076104	
Female	30	19.7035091	
Male	55	26.0065322	
Male	28	22.7738198	
Male	55	33.700649	
Female	61	29.3734273	Thyroxine
Male	44	24.320172	Amlodipine
Female	38	25.3340778	
Female	29	21.4990084	
Female	39	34.5739015	Citalopram
Female	67	27.8703757	
Female	27	21.0824503	
Female	28	21.7854741	Cetirizine
Female	44	28.4945585	Ventolin. Adcal. Gederal (Pill). Clenil.
Female	50	25.4696763	Symbicort. Rhinocort. Loratadine.
Female	71	23.9149369	Thyroxine
Female	55	35.7421875	
Female	27	20.8744247	
Female	24	23.939481	Antibiotics
Female	28	30.1561065	Ventolin. Symbicort.
Male	43	35.6892787	
Female	30	26.384362	
Female	56	25.0291693	
Male	24	28.1748276	
Female	31	21.5163278	Citalopram
Female	62	24.9919323	
Female	34	22.1484375	
Female	26	23.3066801	
Male	41	26.6782007	
Female	33	20.0867749	Cetirizine and Ventolin. Allergy shots

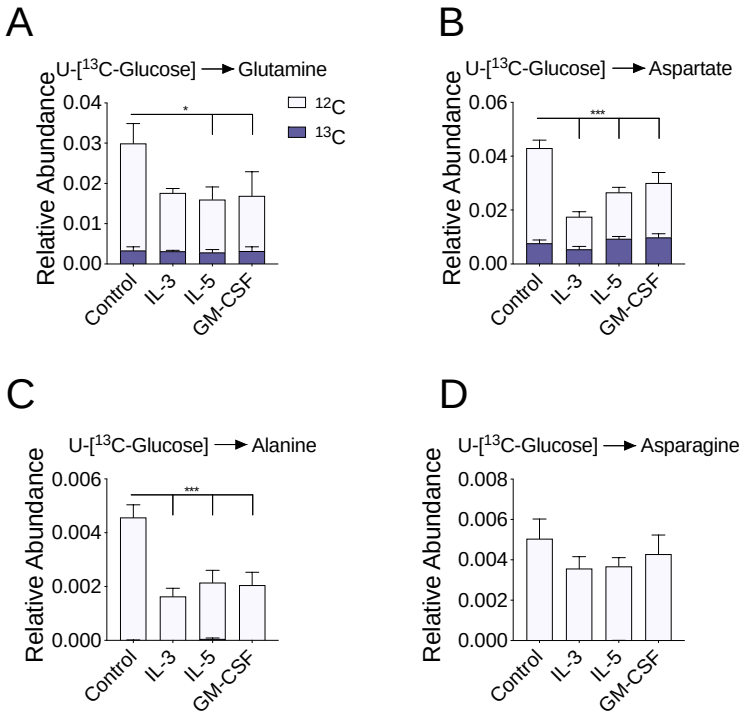
Supplementary Table 1. Demographics of blood donors

Gene Symbol	Gene Name	Primer Sequence	Genbank accession number
SLC2A1 (GLUT1)	Solute carrier family 2 member 1	F - CTATGGGGAGAGCATCCTGC R - CCCAGTTTCGAGAAGCCCAT	NM_006516.2
SLC2A2 (GLUT2)	Solute carrier family 2 member 2	F - TGGAGCTCTCTTGATGGGGT R - ACGATGGCCAGCTGATGAAA	NM_000340.1
SLC2A3 (GLUT3)	Solute carrier family 2 member 3	F - GTGACCTTGCAACTTCATGTC R - AAATGGGACCCTGCCTTACTG	NM_006931.2
SLC2A4 (GLUT4)	Solute carrier family 2 member 4	F - TAGGCTCCGAAGATGGGGAA R - CCCAGCCACGTCTCATTGTA	NM_001042.2
18S	18S ribosomal RNA	F - GGACAGGATTGACAGATTGAT R - AGTCTCGTTCGTTATCGGAAT	NM_000162.3
RPL19	Ribosomal protein L19	F - GCGAGCTCTTTCCTTTCGCT R – TGCTGACGGGAGTTGGCATT	XM_017004061.1

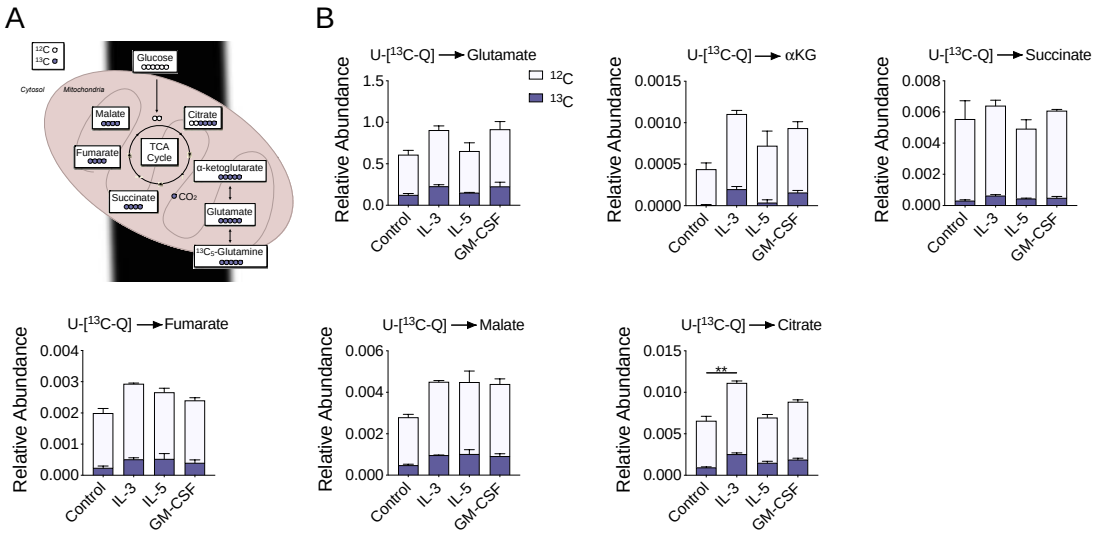
Supplementary Table 2. PCR primer sequences



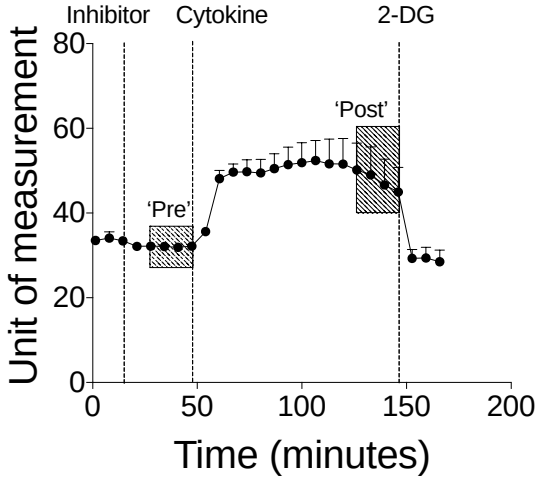
Supplementary Figure 1. Glucose is incorporated into TCA cycle intermediates upon eosinophil activation. Eosinophils were activated for 4 hours with IL-3, IL-5 or GM-CSF (all 10 ng/mL) and the mass isotopic distribution (MID) was analysed for TCA intermediates, (A) citrate, (B) succinate and (C) malate. Data are representative of n = 3 – 6 independent experiments and are expressed as mean + SEM. Statistical analysis was performed using a two-way ANOVA; * $p \leq 0.05$, *** $p \leq 0.001$.



Supplementary Figure 2. Amino acid pools are reduced upon eosinophil activation. Eosinophils were activated with IL-3, IL-5 or GM-CSF (10 ng/mL) for 4 h. Relative abundance of ^{12}C and ^{13}C amino acids, (A) glutamine, (B) aspartate, (C) alanine and (D) asparagine. All data are from 3-6 independent experiments. Data expressed as mean ± SEM. Statistical analysis was performed using a two-way ANOVA; with regards to the ^{12}C data; * $p \leq 0.05$, *** $p \leq 0.001$.



Supplementary Figure 3. Glutamine anaplerosis in IL-3, IL-5 and GM-CSF stimulated eosinophils. (A) Schematic of uniformly labelled $^{13}C_5$-glutamine incorporation into TCA cycle intermediates. Eosinophils were activated with IL-3, IL-5 or GM-CSF (10 ng/mL) for 4 h. (B) Relative abundance of ^{12}C and ^{13}C glutamate, alpha-ketoglutarate, succinate, fumarate, malate and citrate. All data are from 3-4 independent experiments. Data expressed as mean ± SEM. Statistical analysis was performed using a two-way ANOVA; ** $p \leq 0.01$.



Supplementary Figure 4. Example of 'Pre' and 'Post' measurements. Time points used to calculate 'pre' and 'post' measurements.

1. Son K, Mukherjee M, McIntyre BAS, et al. Improved recovery of functionally active eosinophils and neutrophils using novel immunomagnetic technology. *Journal of immunological methods.* 2017;449:44-55.
2. McGuirk S, Gravel SP, Deblois G, et al. PGC-1alpha supports glutamine metabolism in breast cancer. *Cancer Metab.* 2013;1(1):22.
3. Vincent EE, Sergushichev A, Griss T, et al. Mitochondrial Phosphoenolpyruvate Carboxykinase Regulates Metabolic Adaptation and Enables Glucose-Independent Tumor Growth. *Mol Cell.* 2015;60(2):195-207.
4. Jones N, Cronin JG, Dolton G, et al. Metabolic Adaptation of Human CD4+ and CD8+ T-Cells to T-Cell Receptor-Mediated Stimulation. *Frontiers in Immunology.* 2017;8(1516).